© 2020. Published by The Company of Biologists Ltd | Development (2020) 147, dev190066. doi:10.1242/dev.190066

RESEARCH ARTICLE

E93-depleted adult insects preserve the prothoracic gland and molt again

Orathai Kamsoi and Xavier Belles*

ABSTRACT

Insect metamorphosis originated around the middle Devonian, associated with the innovation of the final molt; this occurs after histolysis of the prothoracic gland (PG; which produces the molting hormone) in the first days of adulthood. We previously hypothesized that transcription factor E93 is crucial in the emergence of metamorphosis, because it triggers metamorphosis in extant insects. This work on the cockroach *Blattella germanica* reveals that E93 also plays a crucial role in the histolysis of PG, which fits the above hypothesis. Previous studies have shown that the transcription factor FTZ-F1 is essential for PG histolysis. We have found that FTZ-F1 depletion towards the end of the final nymphal instar downregulates the expression of *E93*, whereas E93-depleted nymphs molt to adults that retain a functional PG. Interestingly, these adults are able to molt again, which is exceptional in insects. The study of insects able to molt again in the adult stage may reveal clues about how nymphal epidermal cells definitively become adult cells, and whether it is possible to reverse this process.

KEY WORDS: Prothoracic gland, E93, FTZ-F1, Ecdysone, Insect metamorphosis, MEKRE93 pathway

INTRODUCTION

One of the most successful innovations in insect evolution is metamorphosis, as shown by the fact that more than 95% of extant insects develop through this type of postembryonic transformation. The simplest mode of metamorphosis, hemimetaboly, originated with the clade Pterygota (viz. the presence of wings), around the middle Devonian, ca. 400 Mya. Subsequently, during the early Carboniferous, ca. 350 Mya, holometaboly evolved from hemimetaboly (Belles, 2019, 2020). Concomitant with the emergence of wings and hemimetabolan metamorphosis is the innovation of the final molt, mainly achieved through histolysis of the prothoracic gland (PG; the gland that produces the molting hormone), which takes place after the winged and reproductively competent adult stage has been reached.

The molecular mechanism that regulates insect metamorphosis is condensed in the MEKRE93 pathway (Belles and Santos, 2014), through which juvenile hormone (JH) becomes bound to its receptor Methoprene tolerant (Met), and induces the expression of Krüppel homolog 1 (Kr-h1); this, in turn, represses the expression of E93. The players most directly involved in regulating metamorphosis are Kr-h1, the transducer of the antimetamorphic signal of JH, and E93, the master trigger of metamorphosis. *E93* was originally discovered as an ecdysone-induced late prepupal-specific gene, during research into histolysis of the salivary glands in *Drosophila melanogaster* metamorphosis (Baehrecke and Thummel, 1995; Lee et al., 2000; Woodard et al., 1994). Subsequently, Mou et al. (2012) found that *E93* is widely expressed in adult cells that form in the pupa of *D. melanogaster*, being required for morphogenesis patterning processes. Further experiments revealed that E93-depleted larvae of *D. melanogaster* are able to pupate but die at the end of the pupal stage. Similar results were observed in the beetle *Tribolium castaneum*, where E93 depletion prevented pupal-adult transition, resulting in the formation of a supernumerary second pupa (Ureña et al., 2014). Moreover, studies on the cockroach *Blattella germanica* have revealed that E93 depletion prevents nymph-adult transition, resulting in reiterated supernumerary nymphal instars (Ureña et al., 2014), and that the expression of *E93* in juvenile nymphs is inhibited by Kr-h1, which closes the MEKRE93 pathway (Belles and Santos, 2014).

Importantly, the MEKRE93 pathway, including the role of E93 as a metamorphosis trigger, is conserved in extant metamorphosing insects (Belles, 2020). This suggests that it was operative in the pterygote last common ancestor. If this is true, then a single mechanism, the MEKRE93 pathway and E93 in particular, might have simultaneously promoted metamorphosis, including wing maturation, and PG histolysis (and hence the final molt) at the origin of the Pterygota (Belles, 2019). The role of E93 as a promoter of metamorphosis and wing maturation has been thoroughly demonstrated (Belles and Santos, 2014; Mou et al., 2012; Ureña et al., 2014; Uyehara et al., 2017). In contrast, nothing is known about the possible role of E93 in PG histolysis. The aim of this work is to explore this possibility using *B. germanica* as a model.

Histolysis of cells and tissues through programmed cell death (PCD) is concomitant with metamorphosis, especially in holometabolans, as new structures are generated and others disappear during this process. In this way, some cells and tissues (such as the salivary glands) disintegrate, whereas others (such as the fat body) undergo remodeling with partial cell replacement (Tettamanti and Casartelli, 2019). Intensive studies based on the larva-pupa transition of *D. melanogaster* have demonstrated the determinant role of ecdysone signaling in PCD processes that affect the salivary glands, midgut and fat body. Ecdysone, or rather its most bioactive derivative 20-hydroxyecdysone (20E), binds the receptor EcR, forms a complex with the coreceptor ultraspiracle (USP) and initiates a gene expression cascade (Hill et al., 2013) that includes *fushi tarazu-factor 1* (*ftz-f1*) and *E93* among the most important genes in the context of PCD (Baehrecke and Thummel, 1995; Broadus et al., 1999). Next, the corresponding proteins promote the expression of PCD genes such as *reaper* (*rpr*) and *head involution defective* (*hid*), as well as caspases and other direct PCD mediators (Jiang et al., 2000; Lee et al., 2000). Other important players are the inhibitors of apoptosis (IAPs), which protect cells and tissues from PCD by preventing caspase activity (Orme and Meier, 2009), although their inhibitory activity on PCD is

Institute of Evolutionary Biology (CSIC-Universitat Pompeu Fabra), Passeig Maritim 37, 08003 Barcelona, Spain.

*Author for correspondence (xavier.belles@ibe.upf-csic.es)

X.B., 0000-0002-1566-303X

Handling Editor: Cassandra Extavour
Received 1 March 2020; Accepted 13 October 2020

Development (2020) 147, dev190066. doi:10.1242/dev.190066

counteracted by Rpr and Hid (Martin, 2002). Therefore, at the larva-pupa transition of *D. melanogaster*, downregulation of *iap1* expression provides the competence for PCD triggered by cell death factors (Orme and Meier, 2009; Yin and Thummel, 2005; Yin et al., 2007).

Although E93 has never been related to PG disintegration, it has been characterized as promoting PCD during metamorphosis in various tissues and species. The first studies, carried out on the salivary glands of *D. melanogaster* and examining the phenotypes of flies with *E93* mutant alleles, indicated that stage- and tissue-specific expression of E93 contributes to their histolysis (Baehrecke and Thummel, 1995; Berry and Baehrecke, 2007; Lee et al., 2000, 2002b; Woodard et al., 1994). More recently, Duncan et al. (2017) reported that mutant alleles of *E93* used in earlier studies in *D. melanogaster* were in fact alleles of a nearby gene *isocitrate dehydrogenase 3b* (*idh3b*), which encodes a key enzyme of the citric acid cycle in mitochondria. Moreover, complete deletion of the *E93* gene did not disrupt cell death, which challenges the previous observations on E93 and salivary gland PCD in *D. melanogaster*. However, the action of E93 on PCD during *D. melanogaster* metamorphosis was reported to occur in the midgut (Lee and Baehrecke, 2001; Lee et al., 2002a) and fat body (Liu et al., 2014), as shown using RNA interference (RNAi) approaches. Finally, following equivalent RNAi approaches, E93 was shown to play the same PCD role in the fat body of the silkworm *Bombyx mori* (Liu et al., 2015).

In *B. germanica*, previous studies revealed that *iap1* expression in the PG declines during the nymph-adult transition, which is followed by PG histolysis. In this cockroach, PG histolysis is regulated by 20E signaling, which leads to a dramatic upregulation of *ftz-f1* expression, whose gene product, FTZ-F1, plays a crucial role in the PCD process (Mané-Padrós et al., 2010). Given the above antecedents, we conjectured that the PCD action of FTZ-F1 on the PG might be mediated by E93. This work confirms the presumption, as FTZ-F1 depletion towards the end of the last nymphal instar downregulates *E93* expression, whereas direct E93 depletion results in adults that retain a functional PG. It was still more intriguing, however, to observe that the E93-depleted adults were able to molt again. Studying this phenotype could provide important clues about how nymphal epidermal cells definitively become adult cells, and whether it is possible to reverse that process.

RESULTS

Tissue-specificity of *E93* expression

We studied the expression pattern of E93 in various tissues involved in metamorphosis, namely the PG, the corpora cardiaca-corpora allata (CC-CA) complex, epidermal tissue (represented by abdominal tergites two to seven) and wing pads. We studied the three most important premetamorphic instars, the fourth (antepenultimate) nymphal instar (N4), the penultimate nymphal instar (N5) and the last nymphal instar (N6). We also measured *ftz-f1* expression given its relationship with PG histolysis. The PG patterns were clearly differentiated from those of other tissues (Fig. 1). The highest expression levels of *E93* in the CC-CA complex, epidermis and wing pads were found towards the middle of N6, whereas in the PG they peak in 8-day-old N6 (N6D8). As for *ftz-f1*, there was a single expression peak in N6D8 in the PG (coinciding with that of *E93*), whereas in the other tissues the expression levels fluctuate as a result of the pulses of 20E that occur around each molt (Fig. 1).

E93 interference late in the last nymphal instar triggers the formation of adults that molt once again

To maximize the depletion of *E93* transcripts in the PG while only minimally affecting the other metamorphic tissues, we injected double-strand (ds)RNA targeting *E93* (dsE93) into N6D6 insects. At this stage, the *E93* expression peak had already elapsed in the CC-CA complex, tergites and wing pads, but was still to come in the PG. Insects injected in N6D6 with either control dsRNA (dsMock) (n=67) or dsE93 (n=132) all molted to adults 2 days later. The control insects showed a normal adult external morphology, with well-shaped and completely extended forewings and hindwings (Fig. 2A). Of the dsE93-treated nymphs, 85.6% molted to adults showing a normal external appearance, with well-shaped and completely extended forewings and hindwings, and 14.4% molted to adults externally normal, but presenting only partially extended wings, particularly the hindwings (Fig. 2A).

We have previously reported that in the adult of *B. germanica* the PG starts disintegrating after the imaginal molt and 3 days later the disintegration is very apparent, with only the axes of muscle, tracheae and nerve of the X-shaped gland, and a few secretory cells, observable (Romaña et al., 1995). In our present RNAi experiments, control adults culminated the histolysis and disintegration process in 3-5 days, whereas the E93-depleted adults retained the integrity of the PG, as observed 8 days after the imaginal molt, when its general morphology resembled that of an N6 PG (Fig. 2B). There was an intriguing difference in cell proliferation: normally, PGs undergo cell division during the first days of N5 and N6 (Kamsoi and Belles, 2019), but we observed no cell division in the PG of E93-depleted adults (Fig. S1).

After the imaginal molt, the E93-depleted adults started to molt again, the first symptoms of which were detected 8 days after the molt to adult, when shadows of the new cuticular structures, including new mandibles, could be observed under the transparent old cuticle. On day 9, the new mandibles were clearly defined (Fig. 2C). One day later, the E93-depleted adults tried to undertake ecdysis, which could not be completed as they were unable to shed the exuvia (Fig. 2D). Even the wings undertook a new apolysis, and a new set of wing veins could be seen under the transparent veins of the E93-depleted adults, being most clearly visible in the forewings (Fig. 2E). Indeed, the vein areas of wings from dsE93-treated insects showed more intense cell proliferation than the controls, as reflected by DAPI staining (Fig. S2).

Molting of E93-depleted adults results from the effective depletion of E93 in the PG, which remains functional

We determined the efficiency of RNAi by measuring the E93 transcript decrease at 48 h after dsRNA injection (i.e. in N6D8). Results showed that *E93* mRNA levels were significantly depleted (ca. 77%) in the PG (Fig. 3A). E93 transcript depletion was also observed in the other tissues studied (CC-CA, tergites and wing pads), although the baseline levels were low, as expected from the expression patterns (Fig. 3A). Simultaneous measurement of *ftz-f1* mRNA levels indicated that E93 depletion did not affect *ftz-f1* expression in the PG, but did trigger a dramatic upregulation in the CC-CA, tergites and wing pads (Fig. 3A). We also observed that the interference of E93 in the late last nymphal instar did not significantly affect the expression in epidermal tissues of *Kr-h1* and *BR-C*, two important genes in adult morphogenesis (Fig. 3B).

We measured the expression of two genes with opposite functions in PG histolysis, *iap1* and *caspase-1* (*casp-1*), on the last day of the last nymphal instar (N6D8) and the first day of the adult stage (AdD1). The results showed that *iap1* expression in N6D8 was significantly higher in E93-depleted insects, although in AdD1 it returned to levels similar to those seen in the controls. In contrast, *casp-1* expression in AdD1 was significantly lower than in the controls (Fig. 3C).

Development (2020) 147, dev190066. doi:10.1242/dev.190066

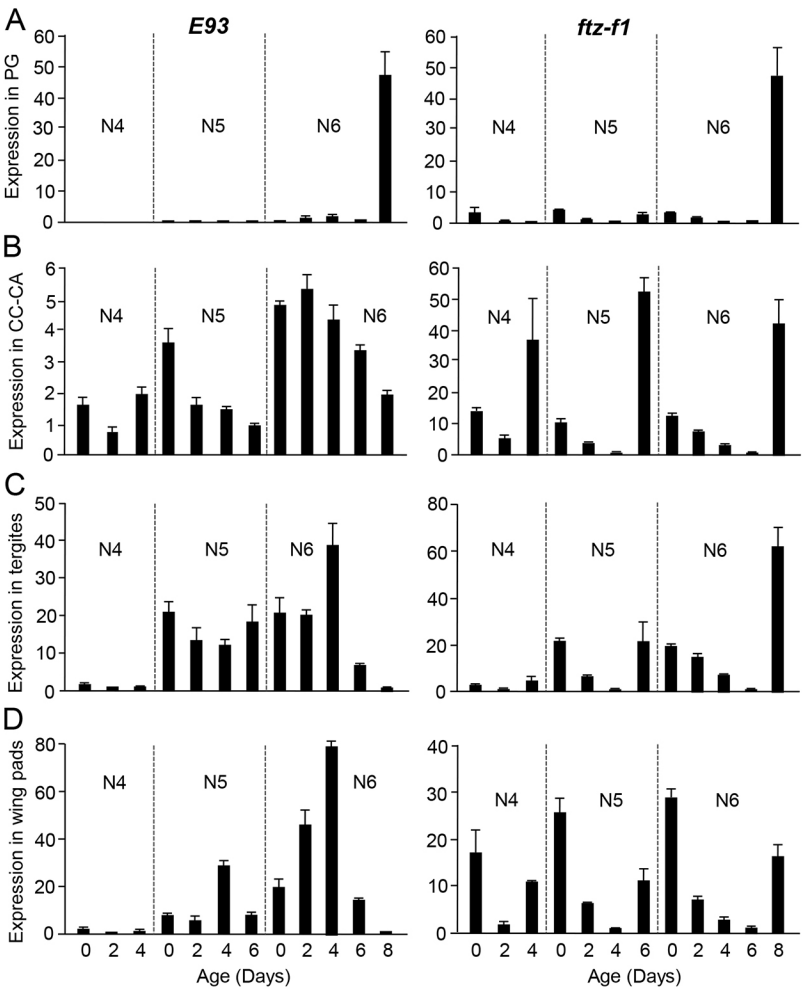

Fig. 1. *E93* and *ftz-f1* expression in the last nymphal instars of *B. germanica*. (A) Expression in the PG. (B) Expression in CC-CA complex. (C) Expression in tergites. (D) Expression in wing pads. Expression was measured during the fourth (antepenultimate) nymphal instar (N4), the fifth (penultimate) nymphal instar (N5) and the sixth (last) nymphal instar (N6) in female insects. The results are indicated as copies of the examined mRNA per 1000 copies of *BgActin-5c* mRNA and expressed as the mean±s.e.m. (*n*=3).

In addition, we measured the expression of the steroidogenic genes *neverland* (*nvd*), *phantom* (*phm*), *disembodied* (*dib*) and *shadow* (*sad*) in the PG of control and E93-depleted 8-day-old adults (AdD8). All these genes were found to be efficiently expressed in the PG of E93-depleted adults, whereas, as expected, expression was very low or undetectable in the controls (Fig. 3D). Consistently, the ecdysone-dependent genes *E75A* and *HR3A* were significantly expressed in the PG of E93-depleted AdD8, suggesting that the gland was producing and was exposed to ecdysteroids, whereas the expression of these two genes was undetectable in the PG of AdD8 controls (Fig. 3E). Indeed, the expression of *E75A* and *HR3A* in the PG of E93-depleted AdD8 was relatively comparable to that measured in untreated N6D6 (Fig. 3E), the age of the last nymphal instar at which the ecdysone pulse is produced (Cruz et al., 2003).

PG death induced by FTZ-F1 is mediated by E93

We have previously reported that FTZ-F1 plays a crucial role in the histolysis of PG in *B. germanica* (Mané-Padrós et al., 2010). Given that E93 depletion in the PG prevented gland histolysis (Fig. 2C), we wondered about the relationships between FTZ-F1 and E93 in the process. As discussed above, E93 appears to repress *ftz-f1* expression in CC-CA, tergites and wing pads, but not in the PG (Fig. 3A). A possible explanation for our observations on the action of E93 and FTZ-F1 on PG histolysis is that FTZ-F1 enhances the expression of E93 in the PG, and that E93 is a more direct gland histolysis effector. To test this conjecture, we treated N6D7 female nymphs (i.e. one day before the peak of *ftz-f1* and *E93* in the PG; Fig. 1) with dsFTZ-F1. We then measured the expression of *E93* (and *ftz-f1*) in the PG. The results showed that RNAi against *ftz-f1* was efficient, as indicated by a significant reduction in the corresponding mRNA levels in the PG (as well as in the CC-CA) at 6 h after dsFTZ-F1 treatment. At 12 h, *ftz-f1* mRNA levels were still decreased in the PG, but the differences with respect to the controls were not statistically significant. Importantly, *E93* mRNA levels were significantly downregulated in the PG at 6 and 12 h, but not in the CC-CA. At 24 h, *ftz-f1* mRNA levels in the PG recovered normal (control) levels, but the significant downregulation of *E93* expression persisted (Fig. 4).

Adults from E93-depleted nymphs have transcriptionally active epidermis and wings

To characterize the type of cuticle synthesized by the adults from E93-depleted nymphs, we first selected typically nymphal or typically adult cuticular proteins (NCPs and ACPs, respectively) from transcriptomic data covering the life cycle of *B. germanica*, which includes N6D6 and AdD5 (GSE99785; Ylla et al., 2018). As NCP genes, we selected *Bg10431*, *Bg10435* and *Bg15257*, which are clearly more expressed in N6 than in adults. *Bg7254* and *Bg16458* were selected as ACP genes, as they are clearly more expressed in adults than in N6 (Fig. S3). The differences between N6 and adults suggested by these transcriptomic data were validated by quantitative real-time PCR (qRT-PCR) measurements (Fig. 5A). Then, measuring the NPC gene expression in AdD5 tergites showed that the levels of *Bg15257* mRNA were similar in controls and in E93-depleted insects,

Development (2020) 147, dev190066. doi:10.1242/dev.190066

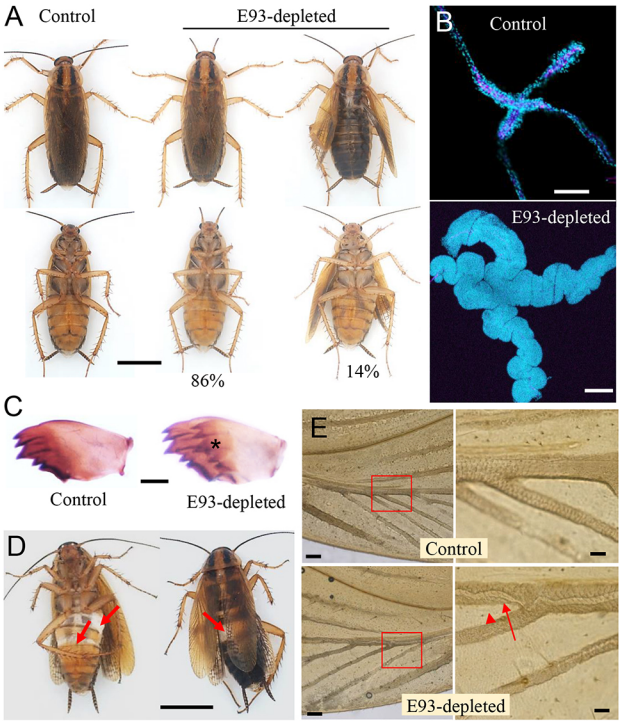

Fig. 2. Effect of *E93* mRNA depletion in the imaginal molt of *B. germanica*. (A) Dorsal and ventral views of control and E93-depleted adults. Sixth instar females nymphs were treated on day 6 with dsMock (control) or dsE93, and the morphology after the imaginal molt was examined. The percentages of E93-depleted adults with extended and unextended wings are indicated. (B) Prothoracic gland of control and E93-depleted adults on day 8 of adult life; the glands were stained with phalloidin (pink) and DAPI (blue). (C) Right mandible of control and E93-depleted adults on day 9 of adult life. Note the new mandible formed under the old one in the E93-depleted adults after apolysis (asterisk). (D) E93-depleted adults attempting to molt on day 10 of adult life; the arrows show areas where the old cuticle separated, showing the new cuticle formed after apolysis. (E) Basal part of the left forewing of control and E93-depleted adults on day 9 of adult life; the part indicated with the red square is shown at higher magnification on the right. Note the new veins (arrow) formed under the old ones (arrowhead) in the E93-depleted adults after apolysis. Scale bars: 5 mm (A,D); 0.1 mm (B); 0.2 mm (C,E, left); 0.05 mm (E, right).

whereas those of *Bg10435* tended to be higher in E93-depleted insects and those of *Bg10431* were significantly higher in E93-depleted insects. The expression levels of the ACP genes were similar in E93-depleted insects and in controls (Fig. 5B).

Next, we wondered about the differences in ecdysteroid signaling in tergites, which could explain why E93-depleted adults molt again and control adults do not. The results showed that the genes encoding the two components of the ecdysone receptor, *EcR* and *RXR*, were similarly expressed in both E93-depleted and control adults. In contrast, expression of the ecdysone-dependent genes *E75A* and *HR3A* was undetectable in control adults, but clearly measurable in E93-depleted adults (Fig. 5C).

Remarkably, wings also showed signs of molting, as indicated by the formation of new veins under the old ones (Fig. 2E). We therefore looked for possible differences in the transcriptional capacity of wings from E93-depleted and control adults. To do this, we measured the expression of the following wing-related genes (Elias-Neto and Belles, 2016) in the hindwings: *blistered* (*bs*), *Notch* (*N*), *Ultrabithorax* (*Ubx*), *scalloped* (*sd*), *nubbin* (*nub*) and *vestigial* (*vg*). For all these genes, the expression was low in the controls, whereas in E93-depleted adults they were four to ten times higher, depending on the gene (Fig. 5D). In all cases, the differences between E93-depleted adults and controls were significant ($P<0.050$), except in the case of *nub* ($P=0.058$), in which the tendency to be upregulated also seemed clear (Fig. 5D).

Treatment with 20E does not trigger molting in control adults

Given that molting of the E93-depleted adults was associated with preservation of the PG and active ecdysone signaling in epidermal cells (Fig. 5C), we wondered whether exogenous administration of 20E to untreated adults might trigger molting. The differences in ecdysteroid titers between nymphs and adults of *B. germanica* are of approximately one order of magnitude. The maximum levels in N6D6 are ca. 2000 pg/µl of hemolymph, whereas in 8-day-old adult females the levels are ca.125 pg/µl (Romaña et al., 1995). Thus, we injected a 0.5 µg dose of 20E in 1 µl volume into 8-day-old adult females (i.e. 2500 pg/µl of hemolymph, close to the physiological concentration in N6D6) ($n=10$). In another equivalent group, we injected the pharmacological dose of 5 µg of 20E in 1 µl volume ($n=10$). The controls received the same volume of solvent ($n=10$). At 8 h after the treatment, three insects of each group were used for qRT-PCR measurements and the remaining insects were kept under observation for at least two weeks. Measurement of *EcR*, *RXR*, *E75A* and *HR3A* expression in tergites showed that neither 20E treatment increased the expression of *EcR* or *RXR*. In contrast, the expressions of *E75A* and *HR3A* were upregulated by 20E in a dose-dependent manner (Fig. 5E). However, even after being treated with 5 µg of 20E, the levels were at least an order of magnitude lower than in 8-day-old E93-depleted AdD8 (Fig. 5C). Importantly, none of the treated adults that we left alive showed symptoms of apolysis.

DISCUSSION

The expression pattern of *E93* and *ftz-f1* in the PG is tissue specific

The expressions of *E93* and *ftz-f1* in the CC-CA, tergites and wing pads in the last nymphal instar of *B. germanica* show a regularly fluctuating pattern, whereas in the PG both genes show a single expression peak on the last day (Fig. 1). The characteristic *E93* and *ftz-f1* expression patterns in various tissues of *B. germanica* have been previously reported (Mané-Padrós et al., 2010; Ureña et al., 2014), but our results show that there is a very peculiar stage- and tissue-specific upregulation of these two genes in the PG, associated with the transition from the last nymphal instar to adult. This PG-specific regulation of *E93* and *ftz-f1* is also suggested by the epistatic relationships between the two genes: E93 does not affect *ftz-f1* expression in the PG but represses it in the other tissues studied (Fig. 3A), whereas FTZ-F1 enhances the expression of *E93* in the PG but not in other tissues such as the CC-CA (Fig. 4).

E93 depletion in the PG prevents its histolysis after the imaginal molt

Given the expression patterns in the different tissues (Fig. 1), injection of dsE93 on the penultimate day of the last nymphal instar had an important effect on E93 in the PG. The result was that the insects molted to adults that were morphologically similar to the controls (Fig. 2A), but their PG did not disintegrate (Fig. 2C). The fact that the PG of the E93-depleted adults did not disintegrate and was fully active was also shown by their active transcription of the steroidogenic genes (Fig. 3D). The significant expression of the ecdysone-dependent genes *E75A* and *HR3A* in the PG of E93-depleted 8-day-old adults (Fig. 3E) also supports the notion that the glands were actively producing ecdysone. It is worth noting, however, that the PG of E93-depleted adults did not present the

Development (2020) 147, dev190066. doi:10.1242/dev.190066

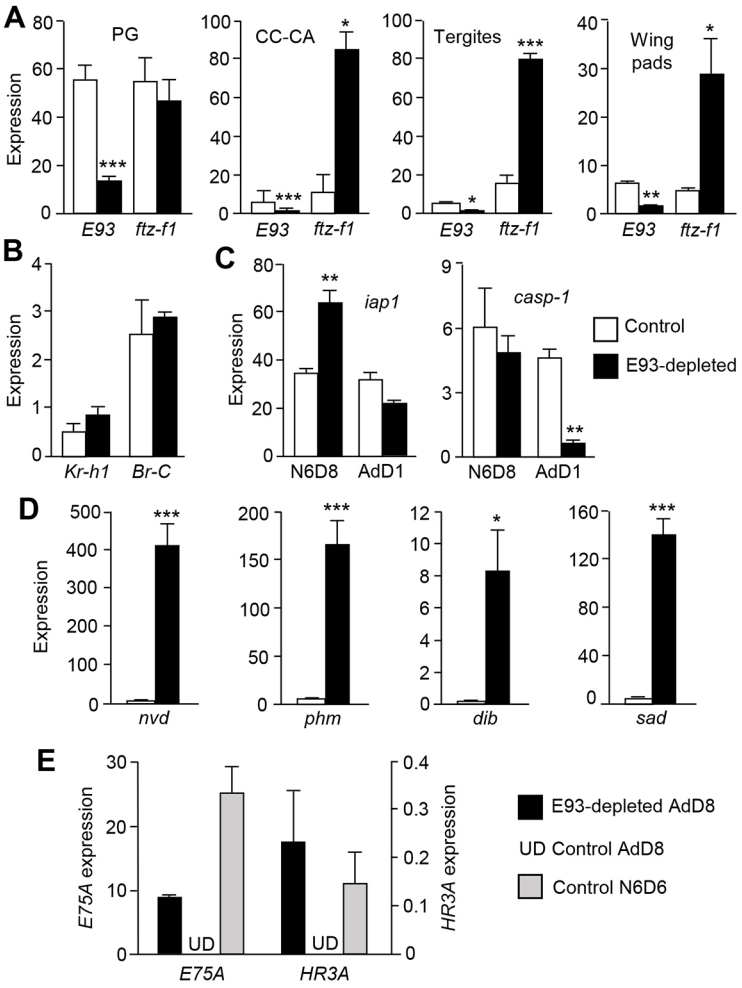

Fig. 3. Effect of E93 depletion on gene expression in *B. germanica*. (A) Expression of *E93* and *ftz-f1* in the PG, CC-CA complex, tergites and wing pads from E93-depleted insects and controls on day 8 of the sixth nymphal instar (N6D8). (B) Expression of *Kr-h1* and *BR-C* in tergites from E93-depleted insects and controls in N6D8. (C) Expression of *iap1* and *casp-1* in the PG of E93-depleted adults and controls in N6D8 and on the first day of the adult stage (AdD1). (D) Expression of the steroidogenic genes *nvd*, *phm*, *dib* and *sad* in the PG from E93-depleted adults and controls in AdD8. (E) Expression of the ecdysteroid signaling genes *E75A* and *HR3A* in the PG from E93-depleted adults and controls in AdD8, and in control nymphs in N6D6. The results are indicated as copies of the examined mRNA per 1000 copies of *BgActin-5c* mRNA and expressed as the mean±s.e.m. (*n*=3). Asterisks indicate statistically significant differences with respect to the controls according to the Student's *t*-test; **P*<0.05, ***P*<0.01, ****P*<0.001; UD, under the detection limit.

typical cell proliferation pattern seen in the first days of nymphal instars (Fig. S1), as observed in untreated N5 and N6 (Kamsoi and Belles, 2019). This suggests that the mechanisms that trigger cell proliferation in the PG at the beginning of each nymphal instar do not operate in the adult stage of E93-depleted insects.

Our observations revealed that E93 depletion kept the expression levels of *iap1* in the PG at the end of the last nymphal instar much higher than in controls. Correspondingly, expression of the effector caspase gene *casp-1* was not upregulated in the PG of E93-depleted insects on the first day of the adult stage (Fig. 3C). These effects of

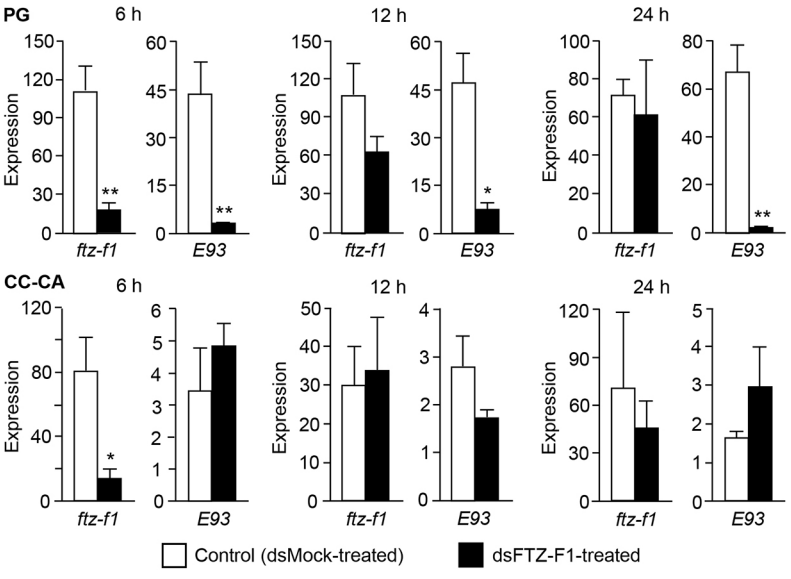

Fig. 4. Effect of FTZ-F1 depletion on *E93* expression in *B. germanica*. Expression of *ftz-f1* and *E93* in PG (top) and CC-CA complex (bottom) at 6, 12 and 24 h after dsFTZ-F1 (or control) treatment in 7-day-old last instar nymphs (N6D7). The results are indicated as copies of the examined mRNA per 1000 copies of *BgActin-5c* mRNA and expressed as the mean±s.e.m. (*n*=3). Asterisks indicate statistically significant differences with respect to the controls according to the Student's *t*-test; **P*<0.05, ***P*<0.01.

Development (2020) 147, dev190066. doi:10.1242/dev.190066

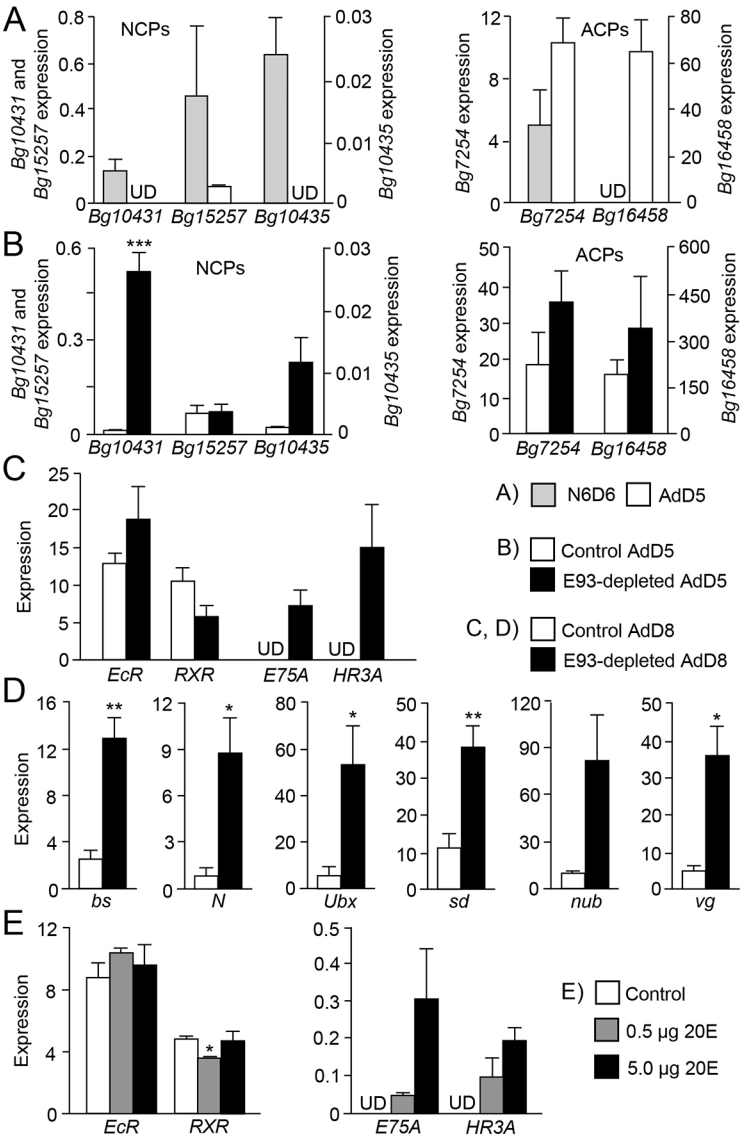

Fig. 5. Effect of *E93* depletion and 20E treatment on gene expression in adult *B. germanica* tissues. (A) Expression of the nymphal cuticular protein (NCP) genes *Bg10431*, *Bg10435* and *Bg15257*, and the adult cuticular protein (ACP) genes *Bg7254* and *Bg16458* in tergites in nymphs on day 6 of the sixth instar (N6D6) and in day 5 adults (AdD5). (B) Expression of the same NCP and ACP genes in tergites of E93-depleted adults and controls in AdD5. (C) Expression of the ecdysteroid signaling genes *EcR*, *RxR*, *E75A* and *HR3A* in tergites of E93-depleted adults and controls on day 8 of adult stage (AdD8). (D) Expression of wing-related genes *blistered* (*bs*), *notch* (*N*), *nubbin* (*nub*), *scalloped* (*sd*), *ultrabithorax* (*Ubx*) and *vestigial* (*vg*) in the hindwings of E93-depleted adults and controls in AdD8. (E) Expression of *EcR*, *RXR*, *E75A* and *HR3A* in adults treated with 20E on day 8 of adult life. The results are indicated as copies of the examined mRNA per 1000 copies of *BgActin-5c* mRNA, and are expressed as the mean±s.e.m. (*n*=3). Asterisks indicate statistically significant differences with respect to the controls; **P*<0.05, ***P*<0.01, ****P*<0.001. UD, under the detection limit.

E93 on the inhibitors and promoters of PCD in the PG provide the mechanistic basis (Martin, 2002; Orme and Meier, 2009; Yin and Thummel, 2005; Yin et al., 2007) for an explanation of why the gland did not disintegrate after the imaginal molt.

E93 triggers PG histolysis

Previous studies revealed that FTZ-F1 depletion prevents PG histolysis in the context of *B. germanica* metamorphosis (Mané-Padrós et al., 2010). Here we show that FTZ-F1 depletion downregulates E93 in the PG (Fig. 4), suggesting that FTZ-F1 enhances the expression of E93 in this gland, which then triggers its histolysis. This activating role of FTZ-F1 on E93 was not observed in other tissues, such as the CC-CA (Fig. 4), where E93 expression declined beyond day 6 of N6 (Fig. 1). The rapid recovery of *ftz-f1* mRNA levels after the injection of dsFTZ-F1 (Fig. 4) is intriguing. Possibly, reaching high levels of FTZ-F1 expression in PG in N6D8 is crucial for undertaking metamorphosis, and the gene response mechanisms to mRNA depletion in this particular tissue and stage are especially efficient (Belles, 2010).

It is known that FTZ-F1 modulates gene expression by interacting with an FTZ-F1 response element (F1RE) located in the target gene promoter (Lavorgna et al., 1991). Interestingly, the promoter region of *B. germanica E93* contains a canonical EcR response element (Cherbas et al., 1991; Kayukawa et al., 2017), as expected, but it also contains the sequence TCAAGGCAA that might be compatible with a F1RE (De Mendonça et al., 2002; Ohno et al., 1994) (Fig. S4). This again suggests that FTZ-F1 co-activates expression of the ecdysone-dependent gene *E93* that occurs in the PG on N6D8, the only stage when FTZ-F1 and E93 co-express at high levels in this gland.

Studies of *D. melanogaster* have previously demonstrated that FTZ-F1 acts as a competence factor during prepupal development, promoting the expression of stage-specific genes such as *E93* (Broadus et al., 1999; Woodard et al., 1994). Moreover, through RNAi experiments, E93 has been shown to promote PCD during metamorphosis in the midgut and fat body of *D. melanogaster* (Lee and Baehrecke, 2001; Lee et al., 2002a; Liu et al., 2014) and in the fat body of *B. mori* (Liu et al., 2015). Therefore, although the PCD function of E93 in the PG in the context of metamorphosis has not been previously reported, this function is not surprising given the above antecedents. The role of E93 as an effector of PG histolysis after the imaginal molt supports the hypothesis that E93 may have been a crucial factor underlying the mechanisms that facilitated the evolutionary innovation of insect metamorphosis (Belles, 2019, 2020).

Development (2020) 147, dev190066. doi:10.1242/dev.190066

E93-depleted adults molt again

Depletion of E93 at the end of the last nymphal instar prevented PG histolysis, but the resulting adults were morphologically normal, in general. Only 14% of them presented partially unextended wings (Fig. 2A), a feature that is not uncommon in control insects. According to the MEKRE93 pathway (Belles and Santos, 2014), the formation of morphologically normal adults is not surprising as the expression levels of *Kr-h1* (and *BR-C*) in the epidermis at the end of the last nymphal instar of E93-depleted insects are as low as in the controls (Fig. 3B). Interestingly, E93-depleted adults are able to molt again, undertaking apolysis, as shown by double structures such as new mandibles, which can be observed under the transparent old cuticle.

Even the wings of these E93-depleted adults undertake apolysis, as shown by the double veins (Fig. 2E), and they are transcriptionally active, according to the high expression levels of wing-related genes (Fig. 5C). The case of *nub* deserves a specific comment, as this gene is activated by E93 in the wing disc of *D. melanogaster* during metamorphosis (Uyehara et al., 2017). The apparent contradiction is explained by the fact that we depleted E93 in *B. germanic*a in N6D6, when the period of maximum expression of E93 in wing pads had already elapsed (Fig. 1). Thus, the metamorphic program in the wings was not altered.

Wing epidermal cells die and disappear after the imaginal molt, and only remain in the wing veins (Kimura et al., 2004). In E93-depleted adults, we observed epidermal cells not only in the veins but also in the intervein regions. Interestingly, the newly formed veins in these adults were bigger than the old ones, thus being folded (Fig. 2E), which fits with the remarkable cell proliferation observed in the vein areas (Fig. S1). The high expression levels of *sd* (Fig. 5D) may have contributed to this proliferation, as this transcription factor acts together with the coactivator Yorkie, regulating Hippo pathway-responsive genes and cell growth and proliferation (Huang et al., 2005; Zhang et al., 2008).

The epidermis of the E93-depleted adults expressed the ACP genes *Bg7254* and *Bg16458* at normally high levels, and those of the NCP gene *Bg15257* at normally low levels for an adult. On the other hand, the genes *Bg10435* and *Bg10431*, which are normally expressed at high levels in the last nymphal instar and at very low levels in the adult, were expressed at remarkably high levels in E93-depleted adults, especially *Bg10431* (Fig. 5B). Thus, from the point of view of cuticular protein expression, the epidermis of E93-depleted adults can be considered fundamentally adult, but with some nymphal character (Fig. 5B). In the epidermis of AdD5 insects, the expression levels of *EcR* and *RXR* were similar in E93-depleted and control insects, but expression of *E75A* or *HR3A* was undetectable in the latter (Fig. 5C). This might suggest that adult controls cannot molt due to low levels of circulating ecdysteroids.

Control adults do not molt even when supplied with 20E

The above conjecture led us to administer 20E to control adults at physiological and pharmacological doses. However, even the pharmacological doses resulted in only a modest increase in *E75A* and *HR3A* expression (Fig. 5E), despite there being operative expression of *EcR* and *RXR* (Fig. 5C). Thus, the treatment did not significantly upregulate *E75A* and *HR3A* expression to the levels observed in E93-depleted AdD8 insects (Fig. 5C), and did not trigger symptoms of molting. This is consistent with classically recorded experiments in moths showing that parabiosis of an adult with a pupa can trigger a molt in the adult (Krishnakumaran and Schneiderman, 1964), whereas injected ecdysteroids very rarely cause molting effects in adults, even when injected in doses as high as 3 mg/g (Schneiderman et al., 1970). In line with these findings, a nymphal active PG implanted into an adult of the Madeira cockroach *Rhyparobia* (=*Leucophaea*) *maderae* can trigger a subsequent molt, even though the insects are unable to undertake the corresponding ecdysis (Engelmann, 2002), just as in our E93-depleted *B. germanica* adults. A possible explanation for the difference between implanted PG and injected 20E is that the implanted PG releases ecdysone according to a precise pattern of increase and decrease that is crucial for triggering the appropriate cascade of gene expression (Sakurai, 2005), which is not reproduced by an injection of 20E. Another possibility, fitting with the adult molt triggered by pupal parabiosis (Krishnakumaran and Schneiderman, 1964) or active PG transplantations (Engelmann, 2002), is the occurrence of PG factors that make the epidermal cells competent to respond to ecdysteroids and produce a new cuticle, a putative factor whose production would be interrupted with histolysis of the PG. Finally, we must consider that the strategy of injecting dsE93 in N6 when the E93 expression peak had already elapsed in most tissues (except PG), maximizes the effects of RNAi in PG while minimizing them in other tissues. However, our RNAi approach has a systemic effect and all tissues are affected, even at a very low level. For example, RNAi also depleted the expression of E93 in CC-CA in N6D8, having produced a concomitant upregulation of the expression of FTZ-F1; this may not produce easily traceable physiological effects in the E93-depleted adult. Whatever the case, these E93-depleted adults that are able to molt again could represent an interesting model in which to study the mechanisms determining the adult differentiation of insect epidermal cells, and perhaps find ways to reverse this process.

MATERIALS AND METHODS

Insects and dissections

The *B. germanica* cockroaches used in the experiments were obtained from a colony fed on Panlab dog chow and water *ad libitum*, and reared in the dark at 29±1°C and 60-70% relative humidity. Prior to injection, dissection or tissue sampling (PG, CC-CA complex, abdominal tergites two to seven, nymphal wing pads and adult wings), the cockroaches were anesthetized with carbon dioxide.

RNA extraction and retrotranscription to cDNA

RNA extractions were carried out with the Gen Elute Mammalian Total RNA kit (Sigma-Aldrich). A sample of 300 ng from each RNA extraction was used for mRNA precursors in the case of nymphal wing pads and abdominal tergites. All the volume extracted from PG, CC-CA complex and adult wings was lyophilized in the FISHER-ALPHA 1-2 LDplus freeze-dryer and then resuspended in 8 µl of milliQ H_2O. RNA quantity and quality were estimated by spectrophotometric absorption at 260 nm in a Nanodrop Spectrophotometer ND-1000 (NanoDrop Technologies). The RNA samples were then treated with DNase (Promega) and reverse transcribed with first Strand cDNA Synthesis Kit (Roche) and random hexamer primers (Roche).

Determination of mRNA levels by quantitative real-time PCR

Measurements with qRT-PCR were carried out in an iQ5 Real-Time PCR Detection System (Bio-Lab Laboratories), using SYBR Green (iTaq Universal SYBR Green Supermix; Applied Biosystems). Reactions were carried out in triplicate, and a template-free control was included in all batches. Primers used to measure the transcripts of interest are detailed in Table S1. The efficiency of each set of primers was validated by constructing a standard curve through three serial dilutions. Levels of mRNA were calculated relative to *BgActin-5c* mRNA (Table S1). Results are given as copies of the examined mRNA per 1000 copies of *BgActin-5c* mRNA.

RNA interference and 20E injections

The detailed procedures for RNAi assays have been described previously (Ciudad et al., 2006). The primers used to prepare the dsRNA targeting *B. germanica* E93 and FTZ-F1 are described in Table S1. The sequence corresponding to the dsRNAs (dsE93 and dsFTZ-F1) was amplified by PCR

and then cloned into a pST-Blue-1 vector. A 307 bp sequence from *Autographa californica* nucleopolyhedrosis virus (Accession number K01149.1) was used as control dsRNA (dsMock). A volume of 1 µl of each dsRNA solution (3 µg/µl for dsE93 and 2 µg/µl for dsFTZ-F1) was injected into the abdomen of sixth instar female nymphs at the chosen ages, using a 5 µl Hamilton microsyringe. Control nymphs were equivalently treated with dsMock. To study the possible molting effect of ecdysteroids in normal adults, 1 µl of a 20E solution (0.5 µg/µl or 5 µg/µl) was injected into the abdomen of 8-day-old adult females with a 5 µl Hamilton microsyringe, whereas controls received 1 µl of solvent (water with 10% ethanol).

Morphological studies

Dissection of PG and adult wings at the chosen ages was carried out in Ringer's saline. The tissues were fixed in 4% paraformaldehyde for 2 h and permeabilized in PBT (0.3% Triton in PBS). PG was first incubated in 300 ng/ml phalloidin-TRITC (Sigma) for 20 min, and subsequently in 1 µg/ml DAPI (Sigma) in PBT for 5 min. In the case of wings, after fixation, they were incubated in 1 µg/ml DAPI for 1 h. After incubation, the tissues were washed three times with PBT, mounted in Mowiol (Calbiochem), and observed with a fluorescence microscope (Carl Zeiss-AXIO IMAGER.Z1). To examine the general morphology, the mandibles and wings were dissected and directly mounted in Mowiol. Examinations and photographs were obtained with a stereomicroscope Zeiss DiscoveryV8.

Experiments to measure cell proliferation in PG

To label DNA synthesis and dividing cells, we followed an approach *in vivo* using the commercial EdU compound Click-it EdU-Alexa Fluor 594 azide (Invitrogen, Molecular Probes). EdU was injected into the abdomen of adults at chosen ages with a 5 µl Hamilton microsyringe (1 µl of 20 mM EdU solution in DMSO). Control specimens received 1 µl of DMSO. The PG from treated specimens was dissected 1 h later and processed for EdU visualization according to the manufacturer's protocol.

Acknowledgements

We thank Jose Carlos Montañes for helping with transcriptome comparisons and searching for genes in the *B. germanica* genome, available at https://www.hgsc.bcm.edu/arthropods/german-cockroach-genomeproject, as provided by the Baylor College of Medicine Human Genome Sequencing Center. We also thank Alba Ventos-Alfonso for helping with different experiments and image treatment, and Maria-Dolors Piulachs and Jose-Luis Maestro for helpful discussions.

Competing interests

The authors declare no competing or financial interests.

Author contributions

Conceptualization: O.K., X.B.; Methodology: O.K., X.B.; Formal analysis: O.K., X.B.; Investigation: O.K., X.B.; Resources: X.B.; Writing - original draft: O.K., X.B.; Writing - review & editing: X.B.; Supervision: X.B.; Project administration: X.B.; Funding acquisition: X.B.

Funding

O.K. received a Royal Thai Government Scholarship to carry out a PhD thesis in X.B.'s laboratory in Barcelona. This work was supported by the Ministerio de Economia y Competitividad (CGL2012–36251, CGL2015–64727-P and PID2019-104483GB-I00 to X.B.), the Consejo Superior de Investigaciones Científicas (2019AEP029), the Generalitat de Catalunya (2017 SGR 1030 to X.B.) and the European Regional Development Fund.

Supplementary information

Supplementary information available online at
https://dev.biologists.org/lookup/doi/10.1242/dev.190066.supplemental

Peer review history

The peer review history is available online at
https://dev.biologists.org/lookup/doi/10.1242/dev.190066.reviewer-comments.pdf

References

Baehrecke, E. H. and Thummel, C. S. (1995). The *Drosophila* E93 gene from the 93F early puff displays stage- and tissue-specific regulation by 20-hydroxyecdysone. *Dev. Biol.* **171**, 85-97. doi:10.1006/dbio.1995.1262

Belles, X. (2010). Beyond Drosophila: RNAi in vivo and functional genomics in insects. *Annu. Rev. Entomol.* **55**, 111-128. doi:10.1146/annurev-ento-112408-085301

Belles, X. (2019). The innovation of the final moult and the origin of insect metamorphosis. *Philos. Trans. R. Soc. B Biol. Sci.* **374**, 20180415. doi:10.1098/rstb.2018.0415

Belles, X. (2020). *Insect Metamorphosis. from Natural History to Regulation of Development and Evolution*. London: Academic Press.

Belles, X. and Santos, C. G. (2014). The MEKRE93 (Methoprene tolerant-Krüppel homolog 1-E93) pathway in the regulation of insect metamorphosis, and the homology of the pupal stage. *Insect Biochem. Mol. Biol.* **52**, 60-68. doi:10.1016/j.ibmb.2014.06.009

Berry, D. L. and Baehrecke, E. H. (2007). Growth arrest and autophagy are required for salivary gland cell degradation in *Drosophila*. *Cell* **131**, 1137-1148. doi:10.1016/j.cell.2007.10.048

Broadus, J., McCabe, J. R., Endrizzi, B., Thummel, C. S. and Woodard, C. T. (1999). The *Drosophila* βFTZ-F1 orphan nuclear receptor provides competence for stage-specific responses to the steroid hormone ecdysone. *Mol. Cell* **3**, 143-149. doi:10.1016/S1097-2765(00)80305-6

Cherbas, L., Lee, K. and Cherbas, P. (1991). Identification of ecdysone response elements by analysis of the *Drosophila* Eip28/29 gene. *Genes Dev.* **5**, 120-131. doi:10.1101/gad.5.1.120

Ciudad, L., Piulachs, M.-D. and Belles, X. (2006). Systemic RNAi of the cockroach vitellogenin receptor results in a phenotype similar to that of the *Drosophila* yolkless mutant. *FEBS J.* **273**, 325-335. doi:10.1111/j.1742-4658.2005.05066.x

Cruz, J., Martín, D., Pascual, N., Maestro, J. L., Piulachs, M. D. and Belles, X. (2003). Quantity does matter. Juvenile hormone and the onset of vitellogenesis in the German cockroach. *Insect Biochem. Mol. Biol.* **33**, 1219-1225. doi:10.1016/j.ibmb.2003.06.004

De Mendonça, R. L., Bouton, D., Bertin, B., Escriva, H., Noël, C., Vanacker, J.-M., Cornette, J., Laudet, V. and Pierce, R. J. (2002). A functionally conserved member of the FTZ-F1 nuclear receptor family from *Schistosoma mansoni*. *Eur. J. Biochem.* **269**, 5700-5711. doi:10.1046/j.1432-1033.2002.03287.x

Duncan, D. M., Kiefel, P. and Duncan, I. (2017). Mutants for *Drosophila* isocitrate dehydrogenase 3b are defective in mitochondrial function and larval cell death. *G3* **7**, 789-799. doi:10.1534/g3.116.037366

Elias-Neto, M. and Belles, X. (2016). Tergal and pleural structures contribute to the formation of ectopic prothoracic wings in cockroaches. *R. Soc. Open Sci.* **3**, 160347. doi:10.1098/rsos.160347

Engelmann, F. (2002). Ecdysteroids, juvenile hormone and vitellogenesis in the cockroach *Leucophaea maderae*. *J. Insect Sci.* **2**, 20. doi:10.1093/jis/2.1.20

Hill, R. J., Billas, I. M. L., Bonneton, F., Graham, L. D. and Lawrence, M. C. (2013). Ecdysone receptors: from the Ashburner model to structural biology. *Annu. Rev. Entomol.* **58**, 251-271. doi:10.1146/annurev-ento-120811-153610

Huang, J., Wu, S., Barrera, J., Matthews, K. and Pan, D. (2005). The Hippo signaling pathway coordinately regulates cell proliferation and apoptosis by inactivating Yorkie, the *Drosophila* homolog of YAP. *Cell* **122**, 421-434. doi:10.1016/j.cell.2005.06.007

Jiang, C., Lamblin, A.-F. J., Steller, H. and Thummel, C. S. (2000). A steroid-triggered transcriptional hierarchy controls salivary gland cell death during *Drosophila* metamorphosis. *Mol. Cell* **5**, 445-455. doi:10.1016/S1097-2765(00)80439-6

Kamsoi, O. and Belles, X. (2019). Myoglianin triggers the premetamorphosis stage in hemimetabolan insects. *FASEB J.* **33**, 3659-3669. doi:10.1096/fj.201801511R

Kayukawa, T., Jouraku, A., Ito, Y. and Shinoda, T. (2017). Molecular mechanism underlying juvenile hormone-mediated repression of precocious larval-adult metamorphosis. *Proc. Natl. Acad. Sci. USA* **114**, 1057-1062. doi:10.1073/pnas.1615423114

Kimura, K.-I., Kodama, A., Hayasaka, Y. and Ohta, T. (2004). Activation of the cAMP/PKA signaling pathway is required for postecdysial cell death in wing epidermal cells of *Drosophila melanogaster*. *Development* **131**, 1597-1606. doi:10.1242/dev.01049

Krishnakumaran, A. and Schneiderman, H. A. (1964). Developmental capacities of the cells of an adult moth. *J. Exp. Zool.* **157**, 293-305. doi:10.1002/jez.1401570302

Lavorgna, G., Ueda, H., Clos, J. and Wu, C. (1991). FTZ-F1, a steroid hormone receptor-like protein implicated in the activation of fushi tarazu. *Science* **252**, 848-851. doi:10.1126/science.1709303

Lee, C. Y. and Baehrecke, E. H. (2001). Steroid regulation of autophagic programmed cell death during development. *Development* **128**, 1443-1455.

Lee, C.-Y., Wendel, D. P., Reid, P., Lam, G., Thummel, C. S. and Baehrecke, E. H. (2000). E93 directs steroid-triggered programmed cell death in *Drosophila*. *Mol. Cell* **6**, 433-443. doi:10.1016/S1097-2765(00)00042-3

Lee, C.-Y., Cooksey, B. A. K. and Baehrecke, E. H. (2002a). Steroid regulation of midgut cell death during *Drosophila* development. *Dev. Biol.* **250**, 101-111. doi:10.1006/dbio.2002.0784

Lee, C.-Y., Simon, C. R., Woodard, C. T. and Baehrecke, E. H. (2002b). Genetic mechanism for the stage- and tissue-specific regulation of steroid triggered programmed cell death in *Drosophila*. *Dev. Biol.* **252**, 138-148. doi:10.1006/dbio.2002.0838

Liu, H., Wang, J. and Li, S. (2014). E93 predominantly transduces 20-hydroxyecdysone signaling to induce autophagy and caspase activity in

Drosophila fat body. *Insect Biochem. Mol. Biol.* **45**, 30-39. doi:10.1016/j.ibmb.2013.11.005

Liu, X., Dai, F., Guo, E., Li, K., Ma, L., Tian, L., Cao, Y., Zhang, G., Palli, S. R. and Li, S. (2015). 20-Hydroxyecdysone (20E) primary response gene *E93* modulates 20E signaling to promote *Bombyx* larval-pupal metamorphosis. *J. Biol. Chem.* **290**, 27370-27383. doi:10.1074/jbc.M115.687293

Mané-Padrós, D., Cruz, J., Vilaplana, L., Nieva, C., Ureña, E., Belles, X. and Martín, D. (2010). The hormonal pathway controlling cell death during metamorphosis in a hemimetabolous insect. *Dev. Biol.* **346**, 150-160. doi:10.1016/j.ydbio.2010.07.012

Martin, S. J. (2002). Destabilizing influences in apoptosis: sowing the seeds of IAP destruction. *Cell* **109**, 793-796. doi:10.1016/S0092-8674(02)00802-4

Mou, X., Duncan, D. M., Baehrecke, E. H. and Duncan, I. (2012). Control of target gene specificity during metamorphosis by the steroid response gene E93. *Proc. Natl. Acad. Sci. USA* **109**, 2949-2954. doi:10.1073/pnas.1117559109

Ohno, C. K., Ueda, H. and Petkovich, M. (1994). The *Drosophila* nuclear receptors FTZ-F1 alpha and FTZ-F1 beta compete as monomers for binding to a site in the fushi tarazu gene. *Mol. Cell. Biol.* **14**, 3166-3175. doi:10.1128/MCB.14.5.3166

Orme, M. and Meier, P. (2009). Inhibitor of apoptosis proteins in *Drosophila*: gatekeepers of death. *Apoptosis* **14**, 950-960. doi:10.1007/s10495-009-0358-2

Romaña, I., Pascual, N. and Belles, X. (1995). The ovary is a source of circulating ecdysteroids in *Blattella germanica*. *Eur. J. Entomol.* **92**, 93-103.

Sakurai, S. (2005). Feedback regulation of prothoracic gland activity. In *Comprehensive Molecular Insect Science* (ed. L. I. Gilbert, K. Iatrou and S. S. Gill), pp. 409-431. San Diego, CA: Elsevier Pergamon.

Schneiderman, H. A., Krishnakumaran, A., Bryant, P. J. and Sehnal, F. (1970). Endocrinological strategies in insect control. *Agric. Sci. Rev.* **8**, 13-25.

Tettamanti, G. and Casartelli, M. (2019). Cell death during complete metamorphosis. *Philos. Trans. R. Soc. B* **374**, 20190065. doi:10.1098/rstb.2019.0065

Ureña, E., Manjón, C., Franch-Marro, X. and Martín, D. (2014). Transcription factor E93 specifies adult metamorphosis in hemimetabolous and holometabolous insects. *Proc. Natl. Acad. Sci. USA* **111**, 7024-7029. doi:10.1073/pnas.1401478111

Uyehara, C. M., Nystrom, S. L., Niederhuber, M. J., Leatham-Jensen, M., Ma, Y., Buttitta, L. A. and McKay, D. J. (2017). Hormone-dependent control of developmental timing through regulation of chromatin accessibility. *Genes Dev.* **31**, 862-875. doi:10.1101/gad.298182.117

Woodard, C. T., Baehrecke, E. H. and Thummel, C. S. (1994). A molecular mechanism for the stage specificity of the *Drosophila* prepupal genetic response to ecdysone. *Cell* **79**, 607-615. doi:10.1016/0092-8674(94)90546-0

Yin, V. P. and Thummel, C. S. (2005). Mechanisms of steroid-triggered programmed cell death in *Drosophila*. *Semin. Cell Dev. Biol.* **16**, 237-243. doi:10.1016/j.semcdb.2004.12.007

Yin, V. P., Thummel, C. S. and Bashirullah, A. (2007). Down-regulation of inhibitor of apoptosis levels provides competence for steroid-triggered cell death. *J. Cell Biol.* **178**, 85-92. doi:10.1083/jcb.200703206

Ylla, G., Piulachs, M.-D. and Belles, X. (2018). Comparative transcriptomics in two extreme neopterans reveals general trends in the evolution of modern insects. *iScience* **4**, 164-179. doi:10.1016/j.isci.2018.05.017

Zhang, L., Ren, F., Zhang, Q., Chen, Y., Wang, B. and Jiang, J. (2008). The TEAD/TEF family of transcription factor scalloped mediates hippo signaling in organ size control. *Dev. Cell* **14**, 377-387. doi:10.1016/j.devcel.2008.01.006

E93-DEPLETED ADULT INSECTS PRESERVE THE PROTHORACIC GLAND AND MOLT AGAIN

Orathai Kamsoi, and Xavier Belles

Institute of Evolutionary Biology (CSIC-Universitat Pompeu Fabra), Passeig Maritim 37, 08003 Barcelona, Spain

Supplementary information

Fig. S1. Cell proliferation in the prothoracic gland of *Blattella germanica*.

Fig. S2. DAPI staining of *Blattella germanica* hindwing in control and E93-depleted adults.

Fig. S3. Transcriptomic expression of typical nymphal cuticular protein (NCP) genes: *Bg10431*, *Bg10435* and *Bg15257* and typical adult cuticular protein (ACP) genes: *Bg7254* and *Bg16458* in *Blattella germanica*.

Fig. S4. The nucleotide sequence of the promoter region of the *E93* gene of *Blattella germanica*.

Table S1. Primers used to measure gene expression levels with qRT-PCR and to prepare dsRNAs for RNAi experiments.

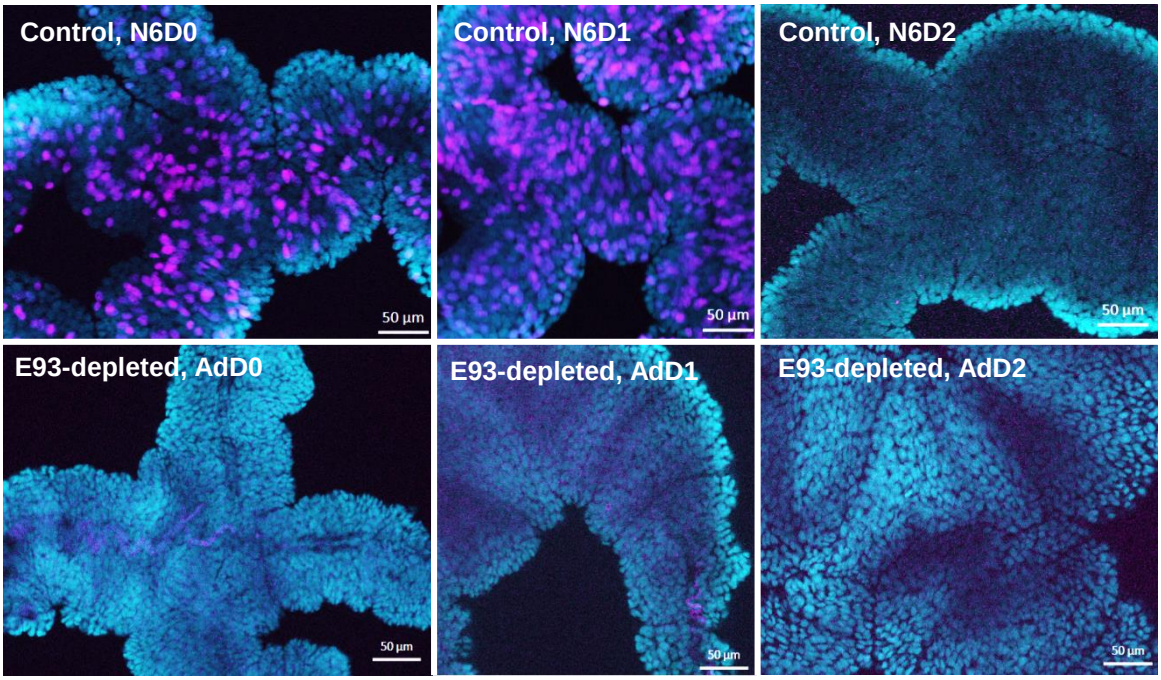

Fig. S1. Cell proliferation in the prothoracic gland of *Blattella germanica*. Double labeling EdU (discrete pink spots) and DAPI (background blue color) of prothoracic gland tissue in last instar control nymphs on day 0 (N6D0), day 1 (NsD1) and day 2 (N6D2), and E93-depleted adults in day 0 (AdD0), day 1 (NsD1) and day 2 (AdD2). Scale bars: 50 µm.

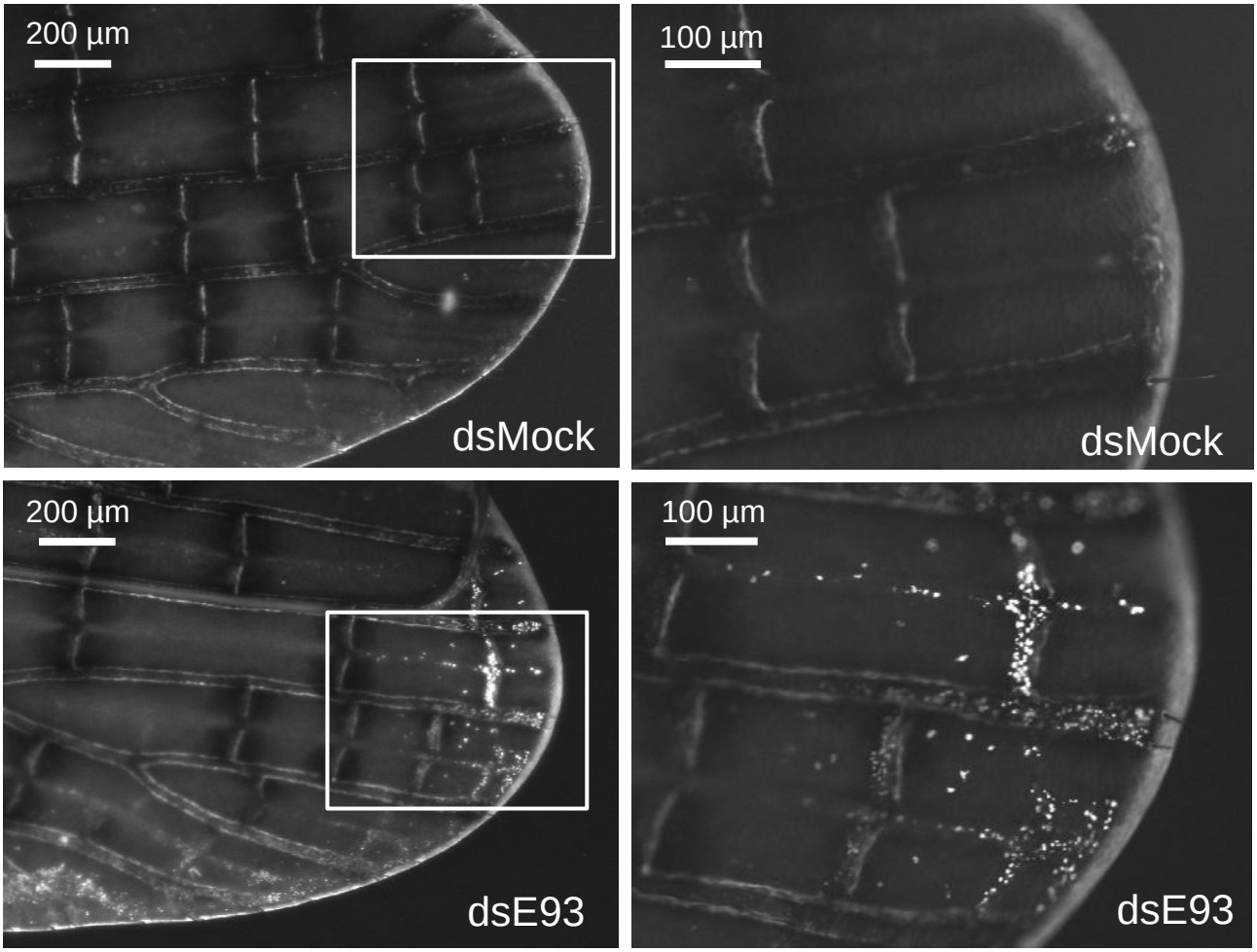

Fig. S2. DAPI staining of *Blattella germanica* hindwing in control and E93-depleted adults. The wings were plucked from 7-day-old adult females, and processed for DAPI staining for 1 h. The images show a general view of the apical part of representative wings, and a detail (white square) at higher magnification. The vein areas of wings from dsE93-treated insects show more intense DAPI staining than controls (dsMock-treated).

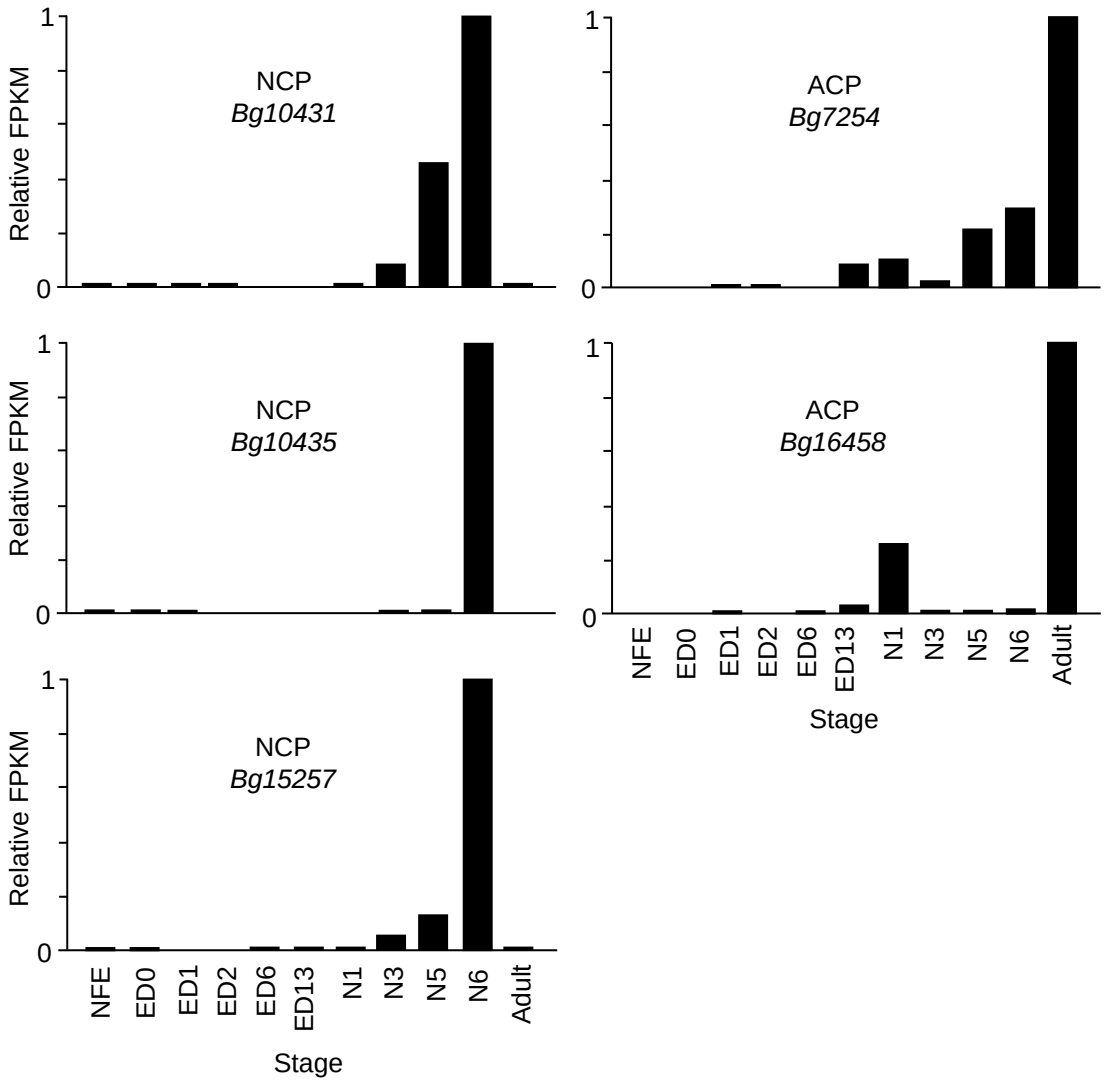

Fig. S3. Transcriptomic expression of typical nymphal cuticular protein (NCP) genes: *Bg10431*, *Bg10435* and *Bg15257* and typical adult cuticular protein (ACP) genes: *Bg7254* and *Bg16458* in *Blattella germanica*. Data were obtained from stage-specific transcriptomes that cover the life cycle (Ylla et al., 2018), as follows: non-fertilized egg (NFE); embryo 8, 24, 48, 144, and 312 h after oviposition (ED0, ED1, ED2, ED6, and ED13); first, third, fifth, and sixth (last) nymphal instar (N1, N3, N5, and N6); adult female. Data are expressed as FPKM, and is normalized against the maximum value (= 1) in each gene.

```
-4010  GGGCCTTCATTACAATAAAATTGTTAGACAATTATTCAGTAATATTTACATAAACAATATTTGTGTCATCAGATAAGATTTATGATACCA
-3920  ATGGCTTTACAAAACTGTCACTAAAGTTTGATTTTATTTATTTATTATTTATTTATTTATCTATCTATTTATTTACAGGTAACTATTTAT
-3830  TTATATATTTATTTATTGTGATATAGAGCTAAGGTCATTGGACCTTCTCTTCCACTCTACCAGCTAAACAAAATTTACAAGATAAATTAC
-3790  ATTATTAAATCAAGTAAAAAGAAAATACAATAAAATTACAAACGAAGTTAAATAAGTTTATCATGAATAACTTTTTGTATTTCCATTGGA
-3710  ATTTCAAACTGTTGTCTTGAATTTTTTTATTTCATACACTCTCTGTGCAGAGCAGAAACATTTTAAACAGCATCATAAAAATACAAGACC
-3620  AGAATTACAATGCAAGATAGTTAAAGATAGTTCTCAAAGGGATGAAACGAAAATATTCCCACTGAAAAAAATATTTATTTGTAGGGATCC
-3530  CTGTTCAGTATTTTAATTTTAATCCAGTCTTTGCTCAGTTTCTTTTCTGATGTTTCTACTCTAGGTGTTACTTATGTTACGGAAGTTAGA
-3440  ATGATAGTTGTAAATAAAATAGCCTACTGCGTTATACTTGTTTATTTTTAAATAAGAATAATGTAATCTCCATCAAATCCCTAAAAAAAG
-3350  AGCTTTCTGCTCTGAGATGTAGACCAGCTAGTTTCTCTGTAGAATAGTTTATCAATAGTACAGTTATATTACCTATATAAATAATAAAAA
-3260  AACGCTTAAATCTCAATAAAGCTCATAATGTCATTATCATGTGGTTGAATTAAAAAGTGTAGATTTTACTGAATGCAGACAACGAGCAAC
-3170  ATAGAGTATAGGACAAACCTGCACAGTGTGAATTGCACTCCGACGTTTACAACGGTCAAAACATTAGTTACTTAATGTCACAAACTTCTA
-3080  ACTCTTCAAGATAGTTAACCTTTTAAAGACTAGCTCCGATATATCGACACTTTCAAGAAGGTTAAAGGGTTAAGAATTAGGTATCTTGCA
-2990  ATATATAAATAACTATAACTAACTGCGTGGTGCAACAGCCCAGCTGTTAGCATTAGGGTCACACATGTCTTAAAATATGGAGGTGAACCA
-2900  TCATCCAACCTGTGAAGGGGAAATATGTGTTTAGCACGTAGAGTCACCAGAAATTAAGCTGTATCTTGCAATCGCCTACAGAAAGGACAG
-2810  AAGAGTTAACTAGACTGCTAAATAAAGTTAAGCTTTACGCAACTTCGCGTCCGCTAGCATAAATCTTCTAATTATGATCGTTCCAAGACA
-2720  GATTAACTCCGTATTTTAAAAGTTAACAACGGGCTATAGCATAAGTTCTTCATGCAGGTAGGCTATGGCATAGGAACAAAATTGGTTGCC
-2630  AACAGTCAAGGCAAATGTCTGGATACTTGTTGAATGCTCAACTTTAGAAGCAGATAAAAGTATAGTCATGTGGAATATTTCGAGAAAATT
-2540  GAGAACAAATATATCTACGAATTCCAAGGAACGTGGGTAATAGATATTAAAGGAATGATGCAGTGGTTGCTTGTCTCTGAACAGAAATCT
-2450  AATAATGGTGTAGTTCAACAATTCAGTTCCTTTTTCTGCCGCATAAACCCGCCATTTTACTGACATACCAAAATAAAAGGTAATTCTGAA
-2360  AACACACTAACTTATTAGTTCAGCTGGTTTTGAACAAAACTGTATTAGCCTATTTATTGCGATGTTTTTGTTAATCTATCGATCACATTA
-2270  TTACCAACCACCTTCTAATTAACTTAATGTAATATGGATTTATAATTACTCTGATAAAAATACCCTTGTCAATAATAATAATAATAATAA
-2180  TAATAATAATAATAATAACCATGTGCCCTTTATGGCTAAGCATCTCCTTTGTCTTTCAGAATTTAATTTTTCATAAATTCAAGGATTAGA
-2090  CTACACCTAGGTATATAGGCAACTTCTTCGACTGTTAAATGTTGCATGTTATCAAAATATTGAAATTGCAGCCCGGACTTCAGAATTGGC
-2000  CGTTTTATTTTCATCAGATACATTATAAATCCATATTACGTTAAGATAATTAGTGGTTAGCTGGTAAAAATAATTACTAACAGCTGCTAA
-1910  GGAATTGGTTGGCACGCTATACAGATTTTGTCAGCATCATCCATCCTAATTCTTTGTTATCAGCAAAGGGACTTTCATTTAAAAGCACCC
-1820  CTCGCACAAATGTACTATAATTTTAAGACTTTGTTCTTGTAACTATGAATACAGAACATAAAATATAATATCAGATCAGAAGGCGATGAA
-1730  CAATTATTATTAATGCAATAATAATGGAATAACTAGATATCGAAACAAAGGTTGATGCTCATGAAAGTCAACAATAAAAGCAATATTATA
-1640  TCCATTTAGCCTACATAGATAAATAACAATTTACTAAAATAATGAAAATGCCATCGAATGCAATGCCACGTGGTAACAATGCTACGGCGG
-1550  AGCAACAGGCGGATTGGGACCCCCGCCCGGTTTAAAGAATGGTGGCATCCGCATCGATTGCGGCGTCGGCCCCACCCTGCGGACAAGACG
-1460  CGAGGATTTTGCAACTTCCCCCTCCCCTCCCTTTCACCCCCGCGACTTTTCTTGTAGCGAGGAAAAACCGAGGCTCCTGCCAGCAAGTTC
-1370  CAAATTCTCCAGAAAATTCTTACATTAATATTTCTCATTCTCATTTTTTTTAATCCTCTCAAAATATTTGTGAATTTCAATCATTCTTCC
-1280  GCATAACATTTAAACTCTTCGGCATTAATTCGGGCAATAAAGGCGTGTTATGATTTAACTCTAAGAAACCGCGTACAGTAGACTATATCA
-1190  ATTTAGAATCAATAGCGCATATTGCTACACTCCTTTGATGTATCTGATTTGAGTTGAACAAATACTTCGGTGTACAAGTGTGGCTTCGCA
-1100  AACTATAGACGTCAGTCATTATAAATATTCCTTCAGGACAACAGTGGGAATCGTGGCCTTCCTCCATTCATTATGAGTGACGACACACGC
-1010  GAGTTGATAGTGCACGGGTGCATCGCAGAGCCAGTGAATCGTACTTATTCTATTACGAAGAAGCGTGTATGTTGCATTCAAGCTCCTTTG
 -920  TTTCTTTAGGAGGATAACGCTAAGGAGTCCTACTACTCGCACGTGAGTCCTAACTCCTGAGGACGCCGCAAGACACGTGACTCGGATCAA
 -830  TACGCCCGTCGTCCCGTCGCGCCGCAGACGTTTGCTATTGATCGACGCCGCGACGCTGCCGCCGGGGATCGATTCCGGACGTCGGAGACG
 -740  AGCGCCGCGTTGCTTGCGCCGCTGTTGCGCGCAGAGGCAGAGCCGGGACTCGAACCCGGGGCGGAGCTCCCCCTCCCGAAAAAAACAGGT
 -650  TTGGGCGTGGCGAAGGCAGCGAGCGGCGGAGAAAAGAGTCAGGGTCAGTTTGCAAGCAAATGGCGGAGTGCTCCTATGCTCGCTGTGTTC
 -560  ACGAGCGACGAGCGATCAAAAAAGAGCTGCAAAGATGGACCAAGAACATGGTGTACGTAGTAGGTGAGTTGTCAAAGTGTGTGTGCTAGT
 -470  GCTCGCGAGGCTGTGGCTCGGCTTAGTGGGCCTCCGCGACCTGTTGCCAAAAAATACGTAAAACAAGGTTCCGGGGTCCCCCTGGTGCAT
 -380  CACCCCGCGTTTCGTGGCGCCCCTGGGTCCTGGGGCCCCCTACGCGCGGGTGCGGGCGTCGCAGTCTTCCGCAAGAAACCCGCTCTGGCC
 -290  GCCCCCGTCAAACATTTCTCAAATTTGGGGCGCATTTTCTCTTCGCGAGCTACCAAACATCAGCTGGTGGGGGGGTGCGTCGCGAGCCTG
 -200  GAACAGCCGGGGCACGAAACGTAACAGCCATGCCATGACCCACCGCAATACCGAGGTAAATACGCGAAAATGGAAAAGTAGGTGAAAATG
 -110  TGACGTGTCGAGCAGCGCGCGAGCAAAGCAGCGGTCGCAGTGTCTTGGGCCCCGAATCCCGATCAGCTTGAGCTTTTGTTGCAGGTCTGG
  -20  AGCGCGTGGCTGAGGAGTTGATGGGCCGCAGAAGATGGAAACAGTATCAGGACTCAGTGCTCAGATCTCCGCTCAGAGTGGACGTGGAGC
```

Fig. S4. The nucleotide sequence of the promoter region of the *E93* gene of *Blattella germanica*. The ATG translation initiation codon is indicated in bold blue, a canonical EcRE (Cherbas et al., 1991; Kayukawa et al., 2017) is indicated in bold green, and a sequence (TCAAGGCAA) compatible with a FiRE (Lavogna et al., 1991; Ohno et al., 1994; de Mendonca et al., 2002) is indicated in bold yellow and underlined, except a mismatched nucleotide. Three other potential FiREs are indicated in yellow and underlined, except the mismatched nucleotides.

Table S1. Primers used to measure gene expression levels with qRT-PCR and to prepare dsRNAs for RNAi experiments (highlighted in yellow).

Gene	Forward primer	Reverse primer	Accession code
Actin 5C (*Act5C*)	AGCTTCCTGATGGTCAGGTGA	TGTCGGCAATTCCAGGGTACATGGT	AJ862721
Bg7254	TTTGTACGGCTACAGCATCG	ACTGACCCAAAGCGTCTTGT	Scaffold293:1224685-1234782*
Bg10431	CTCATGCCGCTCCAGTACTAT	CACGGTAAGACACGACAGGA	Scaffold1062:264085-266425*
Bg10435	CTCTGGTGATGGGCATTTCT	GATTTGCAGAGGAGCAGAGG	Scaffold1062:351421-355992*
Bg15257	AGATCCCTCATGCACCAATC	GCGTGATGTTCAACCTCCTT	Scaffold1678:100341-119028*
Bg16458	GATGGGAGAACCTACCAGCA	CTGGATCTGCGCTAACAACA	Scaffold550:516136-531892*
blistered (bs)	GACGGAGCTCACGTACAACA	CCAGCGGTCTTACTTTCTGC	HF912428.1
Broad-complex (*br*)	CGGGTCGAAGGGAAAGACA	CTTGGCGCCGAATGCTGCGAT	FN651774
caspase-1 (casp-1)	AAGCGGAAGGATTCATACCA	GATGACTGCCTTGCCTCTTC	LN812812.1
disembodied (*dib*)	GCAACAGACAATGGACCTCA	AGATCCAATGCAACCTCCTC	Scaffold1245:376847-417309*
E75A	GTGCTATTGAGTGTGCGACATGAT	TCATGATCCCTGGAGTGGTAGAT	AM238653.1
E93	TCCAATGTTTGATCCTGCAA	TTTGGGATGCAAAGAAATCC	HF536494.1
Ecdysone receptor (EcR)	GACAAACTCCTCAGAGAAGATCAAA	CTCCCAATCCTGCCAGACTA	AM039690.1
fushi tarazu factor1 (ftz-f1)	TTGTCACATCGACAAGACGCA	GTACATCGGGCCGAATTTGTTTCT	CAQ57670.1
HR3A	GATGAGCTGCTCTTAAAGGCGAT	AGGTGACCGAACTCCACATCTC	AM259128.1
inhibitor of apoptosis-1 (*iap1*)	TCCACCTGTGCATCATCATC	GCGTGCATCGTCTAAAACCT	FN668727.1
Krüppel homolog 1 (*Kr-h1*)	GCGAGTATTGCAGCAAATCA	GGGACGTTCTTTCGTATGGA	HE575250.1
neverland (nvd)	CTGGGGCCAGTCACAATACT	GCAGGGGCTTGTCAATGTAT	Scaffold2003:130463-150129*
Notch (N)	GCTAAGAGGCTGTTGGATGC	TGCCAGTGTTGTCCTGAGAG	HF969255.1
nubbin (nub)	CGTCACCAGAAGAAACAACAGA	CGAGATTGTGGTCTGTGAGAAA	LT216433
phantom (phm)	CTAGGCACCAGAGCACCTTC	GCAAGCACTGTGTCTTCCAA	Scaffold1282:295424-296920*
Retinoid X receptor (RXR)	ATAATTGACAAGAGGCAGAGGAA	TGAACAGCCTCCCTCTTCAT	AJ854489.1
scalloped (sd)	GCCCACAGAGTGCTTTCTTC	CCCCTGCCTCATCTTGAATA	HF969263.1
shadow (sad)	ATGAGGAGGTTCAGGGTGTG	CTGGCCAGAAGTCATTTGGT	Scaffold189:1562047-1594901*
Ultrabithorax (Ubx)	AAGAGGTCGCCAGACGTACA	TTGGAACCAAATTTTGATCTGTC	LT216435
vestigial (vg)	AACTGTGTGGTGTTCACTCACT	AAGGAGGGAAGTTGCGAGC	LN901335
dsE93	AAAGAGTTGTCGGGAGCAGA	CCACTGCTAGAAGCCACTCC	HF536494.1
dsFTZ-F1	GAATAGTTCAGGGCTTTTTGAAGCT	GCGACGCATGTGTAGACCTTCTTG	CAQ57670.1
dsMock	ATCCTTTCCTGGGACCCGGCA	ATGAAGGCTCGACGATCCTA	K01149.1

*Genes manually annotated in *Blattella germanica* genome, available as BioProject PRJNA203136.